JOURNAL OF CATALYSIS 118, 498–501 (1989)

Generation of Acid Sites on Finely Divided TiO_2

The generation of new acid sites on mixing oxides was first proposed by Thomas (*1*) and further developed by Tanabe and co-workers (*2*). Recently, Connell and Dumesic (*3*) have studied the generation of new acid sites on a silica surface by the addition of several kinds of dopant cations. There seems to be a common idea in these works that the generation of new acid sites is ascribed to the charge imbalance at locally formed $M(1)$–O–$M(2)$ bondings, where $M(1)$ is the host metal ions and $M(2)$ the doped and/or mixed metal ions. The charge imbalance might be expected even on single-component metal oxides consisting of small particles, since the electronic properties of small-sized metal or oxide particles are widely accepted to be somewhat different from those of the bulk materials (*4*). These differences are partially attributed to the surface imperfections of crystallographic structures in small-sized particles. Typical imperfections in small particles are metal or oxygen vacancies, causing the local charge imbalance. Thus, the purpose of the present work is to discuss the relationship between particle size and surface acidity of metal oxides.

Titanium dioxide was used as a model oxide and was prepared by the hydrolysis of titanium tetraisopropoxide (Kojundo Kagaku CO., 99.9% purity) dissolved in propyl alcohol. Hydrolysis was carried out as follows: 0.025 mol of the alkoxide was first dissolved in 50 ml of propyl alcohol and the solution was then slowly poured into distilled water with vigorous stirring. The amount of distilled water was varied from 0.05 to 5.0 liters with the aim of controlling the size of the resultant TiO_2 particles. The precipitates thus prepared were dried at 110°C, followed by calcination at 420°C for 3 h in air. All the powders thus produced were anatase and no trace of rutile was detected by X-ray diffraction measurements (anatase is reported to transform to rutile only at temperatures higher than 600°C) (*5*). BET surface areas and mean particle sizes estimated by both X-ray line broadening using the Scherrer equation and a transmission electron microscope (TEM, Hitachi H-800) are given in Table 1. The TEM was operated at an accelerating voltage of 200 kV with a magnification of $\times 10^5$ and photographs were enlarged twice when printed. Typical photographs are shown in Fig. 1.

The particle size distribution curves were obtained by means of small-angle X-ray scattering (SAXS, Rigakudenki Co., Geigerflex) equipped with a scintillation counter fitted with a line-focused Cu X-ray tube (60 kV, 200 mA) using a Ni filter (*6*). The scattered X-rays were scanned at a 2θ-per-min rate of 0.025 over the range $0.1 < 2\theta < 3.5$. The scattering from micropores in TiO_2 powders was roughly eliminated by use of diiodomethane as a pore-masking agent, although the electron density of TiO_2 is a little larger than that of the masking agent. The sample powders were evacuated at 200°C for 1 h before the adsorption of the maskant vapor at room temperature. From the intensity curves plotted as a function of diffraction angle, the Guinier (R_G) and Porod (R_P) radii were calculated according to the equations given by Whyte *et al.* (*7*) and are shown in Table 1. These parameters were used to plot the particle size distribution curves with an assumption of lognormal distribution (*7*) and the results obtained are depicted in Fig. 2.

The sample powders were calcined at

0021-9517/89 $3.00

TABLE 1

BET Surface Areas and Mean Particle Sizes Obtained by X-Ray Line Broadening and TEM, with Parameters of R_G and R_P Estimated from SAXS Measurements

Sample no.	Water added (ml)	Surface area (m^2/g)	Size by XRD (Å)	Size by TEM (Å)	Size by SAXS			Highest acid strength (H_0)
					$2R_G$ (Å)	$2R_P$ (Å)	Av. (Å)	
A	5000	335	43	55	53	49	55	−5.6
B	2000	140	60	65	70	69	65	−3.0
C	1000	105	125	180	229	220	210	1.5
D	300	94	125	192	314	262	220	3.3
E	50	81	160	254	413	367	330	4.0
F	Commercial	39	410	1500–2300	—	—	—	4.8

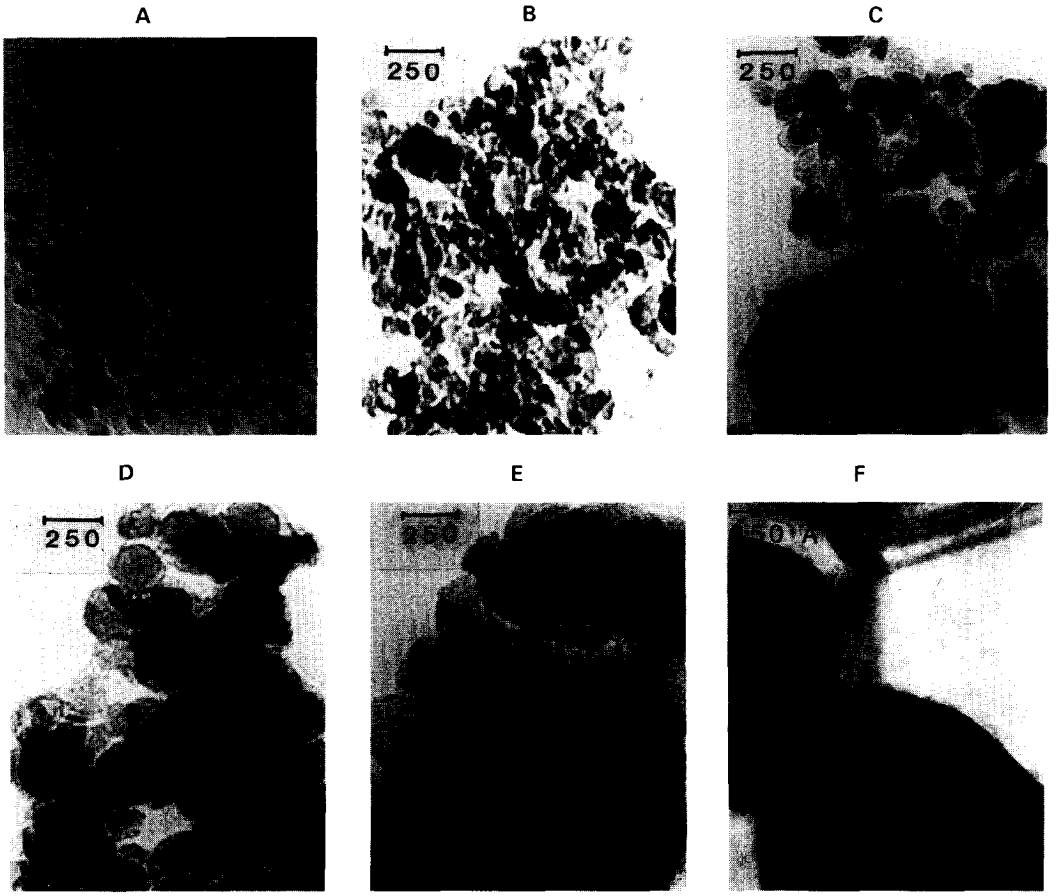

FIG. 1. Typical TEM micrographs of TiO_2 particles prepared by hydrolysis of Ti tetraiso-propoxide. Amounts of (a) 0.5, (b) 0.1, (c) 1.0, (d) 2.0, and (e) 5.0 liters of distilled water were employed for hydrolysis. A commercial TiO_2 was used in (f). Bar indicates 250 Å.

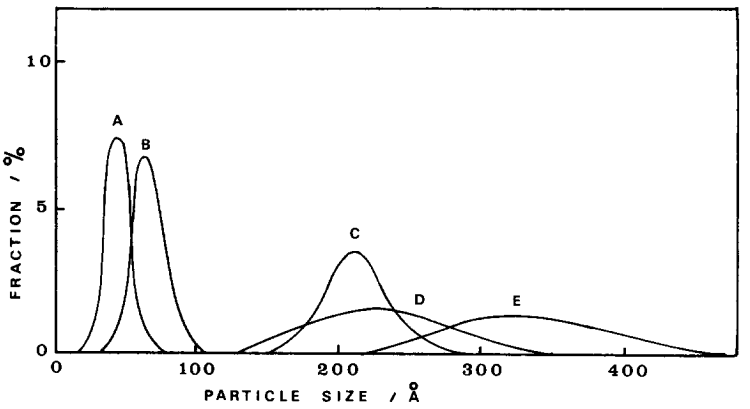

FIG. 2. Particle size distributions obtained by SAXS; notations are the same as those given in Fig. 1.

350°C for 1 h in flowing oxygen and then evacuated at the same temperature for 30 min before being submitted to the titration tests to determine their acidities. Although the highest acid strength was definitely determined by observation of the changes in color of the indicators, attempts to measure the number of acid sites by titration were unsuccessful because of indistinct endpoints of the titration. Accordingly, only the highest acid strengths were plotted against the mean particle sizes of TiO_2 employed (Fig. 3). The indicators used here are effective for detecting both Brønsted and Lewis acid sites and are listed in Table 2 together with their pK_a values.

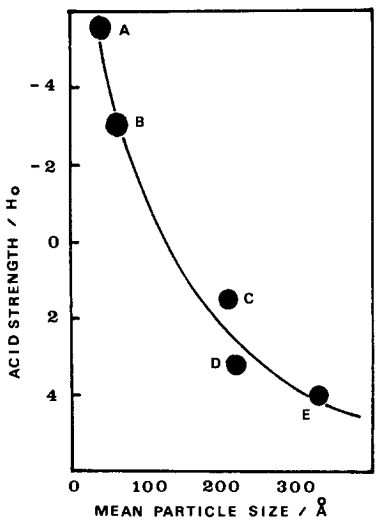

FIG. 3. Relationship between particle size and the highest acid strength of TiO_2 particles; notations are the same as those given in Fig. 1.

The highest acid strength apparently increases with a decrease in the particle size, indicating the generation of new and strong acid sites on small-sized TiO_2 particles. Consequently, even on the single-component oxides, i.e., even with the absence of new $M(1)$–O–$M(2)$ bonding, new and strong acid sites are generated when the oxide powders are composed of finely divided particles. This is likely to be due in this case to the presence of many oxygen vacancies existing on the surface of small-sized TiO_2 particles, since TiO_2 is considered to be an *n*-type semiconductor. The oxygen vacancies generate considerable numbers of dangling bonds, whose energy levels are located in the bandgap region between the valence and the conduction bands. Elec-

TABLE 2

Indicators Employed and Their pK_a Values

Indicators	pK_a
1-Phenylazo-2-naphthylamine	4.0
p-Dimethylaminoazobenzene	3.3
Benzeneazodiphenylamine	1.5
Dicinnamalacetone	−3.0
Benzalacetophenone	−5.6

trons trapped in these levels probably cause the local charge imbalances, and hence the generation of new and strong acid sites over the surface of finely divided TiO_2 particles.

REFERENCES

1. Thomas, C. L., *Ind. Eng. Chem.* **41,** 2564 (1949).
2. Tanabe, K., and Takeshita, T., *in* "Advances in Catalysis" (D. D. Eley, P. W. Selwood, and Paul B. Weisz, Eds.), Vol. 17, p. 315. Academic Press, New York, 1967; Tanabe, K., "Solid Acids and Bases." Academic Press, New York, 1970.
3. Connell, G., and Dumesic, J. A., *J. Catal.* **102,** 216 (1986); **105,** 285 (197).
4. Anderson, J. R., "Structure of Metallic Catalysts." Academic Press, New York, 1975.
5. Shannon, R. D., and Pask, J. A., *J. Amer. Chem. Soc.* **77,** 391 (1965).
6. Ueno, A., Suzuki, H., and Kotera, Y., *J. Chem. Soc. Faraday Trans. 1* **79,** 127 (1983).
7. Whyte, T., Kirklin, P., Gould, R., and Heinemann, H., *J. Catal.* **25,** 407 (1972).

KATSUHIKO NISHIWAKI
NORIYOSHI KAKUTA
AKIFUMI UENO

Department of Materials Science
Toyohashi University of Technology
Tempaku, Toyohashi, Aichi 440, Japan

HIROTOSHI NAKABAYASHI

Department of Chemistry
Kochi Technical College
Monobe, Nangoku, Kochi 783, Japan

Received April 13, 1988; revised March 1, 1989